Asian Journal of Chemistry; Vol. 37, No. 9 (2025), 2115-2122
ASIAN JOURNAL OF CHEMISTRY
https://doi.org/10.14233/ajchem.2025.33949

Polymer-Magnetite Nanocomposite as a Promising Multifunctional Additive for Lubricating Oil

LEIYAMI AHUNGSHI[1], and MAINUL HOQUE[2,*],

[1]Department of Chemistry, Bodoland University, Kokrajhar-783370, India
[2]Department of Chemistry, Kokrajhar Government College, Kokrajhar-783370, India

*Corresponding author: E-mail: mainulkgc@gmail.com

Received: 29 April 2025 *Accepted*: 25 June 2025 *Published online*: 30 August 2025 AJC-22090

Polymer nanocomposites have garnered significant attention in the lubricant industry due to their superior properties compared to unmodified polymers. In this research, the magnetite (Fe_3O_4) nanoparticles was synthesized and subsequently incorporated into castor oil-based polymers at varying concentrations. The resulting nanoparticles and polymer/nanocomposites were characterized using various analytical techniques. Their performance as viscosity index improver, pour point depressant and anti-wear properties were assessed by blending them with a mineral base stock in different proportions. Standard ASTM procedures were employed for these evaluations. The findings revealed that increasing the nanocomposite content in the base stock significantly enhanced the overall performance of the formulated lubricant.

Keywords: Castor oil, Magnetite nanoparticles, Pour point depressant, Viscosity index improver, Anti-wear properties.

INTRODUCTION

In today's context of energy scarcity, friction and wear have become critical areas of concern. A study by Holmberg & Erdemir [1] reveals that tribological contacts are responsible for approximately 23% of global energy losses, with the majority of this energy being consumed in overcoming friction. Friction and wear in mechanical components are the major contributors to energy efficiency loss and equipment failure. They also result in significant environmental pollution and substantial economic losses, making it a critical issue that requires urgent attention in today's world [2]. To combat friction and wear, enhance energy efficiency, protect the environment and boost machinery performance, lubrication serves as one of the most effective strategies [3].

Lubricants are widely used in the automotive industry as they create a protective layer on machinery surfaces, reducing friction during turbo-chemical processes. In addition to that, it enhances engine efficiency, extends their lifespan and helps save energy. It has been observed that certain inorganic additives exhibit superior extreme pressure properties compared to some organic additives [4]. Unfortunately, the insolubility and challenges in achieving a stable dispersion of inorganic powders limit their use in lubricating oils. The use of oil-soluble additives as effective friction reducers and anti-wear agents has been widely explored in lubrication engineering in recent decades [5]. However, the use of these additives leads to the increased pollution, toxicity and environmental waste disposal issues.

The use of nanomaterials as additives helps overcome these limitations and creates new possibilities in the lubricant industries [6,7]. Nanoparticles have been added to the lubricating oils to enhance their tribological properties. In recent years, numerous studies have explored the effectiveness of various inorganic nanoparticles in reducing friction and wear in lubricating oils [8-10]. Due to their outstanding tribological properties and eco-friendly nature, nanoparticles have become a preferred alternative to traditional lubricating oil additives, especially under conditions of high load, high sliding speed and elevated friction [11,12]. The nanoparticles adhere to the friction surfaces, leading to changes in these surfaces and enhancing their tribological properties. Copper nanoparticles have gained significant attention due to their exceptional properties [13]. They can greatly enhance the tribological properties of lubricating oil [14]. The addition of graphite nanosheet as additives to lubricating oil enhances

the tribological properties of paraffin oil [12]. The addition of MoS_2 nanoparticles greatly enhanced the load-carrying capacities and anti-wear properties of paraffin oil [15,16]. The oxide-based nanoparticles like CuO nanoparticles, demonstrate effective anti-wear and friction-reducing properties [17]. Studies on coatings containing CeO_2, TiO_2 and TiS_2 have demonstrated that they offer effective friction reduction and anti-wear properties along with outstanding anti-wear [18] have been produced. The nanoparticles mentioned above are non-magnetic under normal conditions and offers practical advantages in lubricant design, especially in terms of dispersion stability, tribochemical film formation and thermal endurance. Furthermore, the use of non-magnetic compounds, such as those containing sulfur, phosphorus, lead and other elements, as antifriction additives in lubricants can have negative environmental impacts [19].

Magnetic nanoparticles being environmentally friendly, has gained significant interest in this field. One of the key benefits of using magnetic nanoparticles as lubricant additives is their magnetic properties, which stem from their remanent magnetization [20]. The lubricant containing Fe_3O_4 nanoparticles creates a protective film that adheres to the frictional steel surfaces, filling in gaps and cracks. This is due to the potential magnetic interactions between the lubricant and the friction surface, as well as tribo-chemical reactions occurring on the metal surface [21,22]. This leads to a notable enhancement in the anti-wear properties of the lubricating oil. Huang *et al.* [23] investigated the impact of magnetite nanoparticles on the tribological properties of paraffin oil, finding that the addition of nanoparticles enhanced the load-carrying capacity and anti-wear characteristics of the lubricant when compared to pure paraffin oil. Xiang *et al.* [24] examined the tribological and tribo-chemical characteristics of magnetite (Fe_3O_4) nano-flakes when used as an additive in mineral base fluids. The discussion reveals that magnetite nanoparticles, along with other oxide-based nanoparticles, are utilized solely as anti-wear and friction reducing additives in lubricating oils. In addition, acrylate-based polymers are recognized for their effectiveness as viscosity index improvers (VII) [25-27] and pour point depressants (PPD) [28]. There is a limited amount of research on vegetable-oil-based polymers known for their tribological characteristics. Therefore, to introduce a multifunctional capability (combining VII, PPD, anti-wear and friction reduction) into lubricant additives, this research proposed creating polymer nanocomposites of castor oil using magnetite (Fe_3O_4) nanoparticle as fillers.

EXPERIMENTAL

Castor oil with a high unsaturation rate of 96.7% was sourced from a local grocery [29]. Benzoyl peroxide with 98% purity supplied by LOBA Chemie in India, was recrystallized using a chloroform-methanol ($CHCl_3$-MeOH) mixture before use. While base oil SN150 was collected from the Indian Oil Corporation Limited (IOCL) in Dhakuria, India. Iron(II) sulphate heptahydrate (purity > 99%), potassium nitrate and potassium hydroxide (99.9%) were obtained from Merck Specialties Pvt. Ltd. Cetyltrimethyl ammonium bromide (CTAB) was obtained from Sisco Research Laboratories and toluene was obtained from LOBA Chemie with 99% purity.

Synthesis of polymer (homopolymer): The process for synthesizing a homopolymer from castor oil in different ratios was conducted in a three-necked round-bottom flask outfitted with a mechanical stirrer, condenser, thermometer and a nitrogen inlet, without the use of a solvent. Initially, the mixture was stirred at 50 ºC for 30 min to obtain a homogeneous solution. Benzoyl peroxide (BZP) was then added as an initiator. The polymerization took place through a free radical process at 90 ºC for 6 h. Following the reaction, the mixture was transferred into methanol with continuous stirring to stop polymerization and to precipitate the polymer. The resulting polymers were purified by multiple precipitation cycles from a hexane solution using methanol and subsequently dried under vacuum at 40 ºC [30,31].

Synthesis of magnetite (Fe_3O_4) nanoparticles: Magnetite nanoparticles was prepared using the reported method of Bruce *et al.* [32]. A solution of iron(II) sulphate heptahydrate (1.67 g, 6×10^{-3} mol) was dissolved in 50 mL of deionized water, while KNO_3 (1.01 g, 1×10^{-2} mol) was dissolved in 10 mL of deionized water. Furthermore, 2.5 M KOH solution was prepared followed by the addition of the surfactant CTAB 1% (w/w) was added to the iron salt solution, which was then vigorously stirred for 2 h. A solution of potassium nitrate was added to the mixture and stirred for an additional 30 min. Then, 10 mL of 2.5 M KOH (containing 2.5×10^{-2} mol) was gradually introduced. The reaction mixture was subsequently heated to 100 ºC under a nitrogen atmosphere and maintained at this temperature for 2 h. Afterward, the nitrogen flow was stopped and the mixture was allowed to cool to room temperature. Once cooled, the black precipitate was thoroughly washed with deionized water, centrifuged and then dried under vacuum at 323 K overnight [33].

Synthesis of polymer-Fe_3O_4 nanocomposites: Polymer -Fe_3O_4 nanocomposites was synthesized by mixing the prepared polymer and Fe_3O_4 nanoparticles with a toluene solution. To prepare the polymer-Fe_3O_4 suspension, 6 g of polymer were dissolved in toluene and the required amounts (0.01, 0.02 and 0.03 g) of Fe_3O_4 nanoparticles were added under ultrasonic treatment with continuous stirring. The resulting suspension was poured onto a glass plate, allowing the toluene to evaporate naturally, which resulted in a semi-solid polymer-nanocomposite mass and then characterized [34].

Characterization: The polymers were characterized using a BRUKER AVANCE II 400 MHz FT-NMR spectrometer. Infrared (IR) spectra were recorded on a Shimadzu FT-IR 8300 instrument with 0.1 mm KBr cells at room temperature, spanning the range of 4000-400 cm^{-1}. For ^1H NMR analysis, 5 mm broad band observe (BBO) probes were employed with DMSO serving as the reference solvent.

Determination of average molecular weight by GPC method: The SEC-GPC system was utilized to measure the number average molecular weight (M_n), weight-average molecular weight (M_w) and polydispersity index (PDI) of the synthesized polymers. This GPC set up, calibrated with polystyrene standards, included a 2414 refractive index detector, a Waters 515 HPLC pump, a 717 Plus autosampler

and a 2489 UV/Visible detector. HPLC-grade THF was employed as the eluent, flowing at a rate of 1.0 mL/min, with the system maintained at 30 ºC. Table-1 presents the average molecular weight values obtained from the GPC analysis [35]. The thermal stability of the polymer was assessed using a Shimadzu TGA-50 system. The analysis was performed in an alumina crucible with a heating rate of 10 ºC per min in an air atmosphere. The Fe_3O_4 nanoparticles and their composites were analyzed using a field emission scanning electron microscope (FE-SEM, INSPECT F50, FEI), a transmission electron microscope (TEM) and X-ray diffraction (XRD, Advance D8, Bruker) [34].

TABLE-1
MOLECULAR WEIGHT OF THE PREPARED POLYMER (M_n, M_w AND PDI VALUE)

Polymer sample	M_n	M_w	PDI
P	2277	2729	1.198

P: 100% of CO, M_n: Number average molecular weight, M_w: Weight average molecule, PDI: Polydispersity index

Viscosity index determination: The viscosity index (VI) is a dimensionless qualitative measure that indicates the extent to which the viscosity of base oil varies with temperature. The viscosity index (VI) of the polymeric additive was measured in a paraffinic base oil to assess the effectiveness of the additive as viscosity modifier (VM). The VI of the base oil mixed with the additive at various concentration levels was determined following the ASTMD 2270 method, using the equations as outlined by Tanveer & Prasad [36].

Determination of pour point: The pour point depressant properties of base oils blended with polymeric additive was evaluated by measuring the pour points of the lubricants using a Cloud and Pour Point Tester (Model WIL-471, India) following the ASTM D97 standard method. For each sample, varying concentrations of the additives, ranging from 1% to 4% (w/w) were tested.

Evaluation of anti-wear property: The anti-wear properties of the lubricant compositions with additives at different concentrations ranging from 1% to 4% were evaluated using a Four-Ball Wear Test (FBWT) apparatus in accordance with the ASTM D 4172-94 standard. The test involved applying a load of 392 N (40 kg) at a temperature of 75 ºC for duration of 30 min to measure the wear scar diameter (WSD). The test balls had a diameter of 12.7 mm and the rotation speed was maintained at 1200 rpm [30,37].

RESULTS AND DISCUSSION

FTIR studies: The FT-IR spectra of homopolymer (a) and homopolymer/Fe_3O_4 nanocomposite (b) are presented in Fig. 1. In Fig. 1a, the absorption band observed at 1739.40 cm^{-1} corresponds to the ester carbonyl stretching vibration of polymer. In Fig. 1b, the absorption peak at 1734 cm^{-1} represents

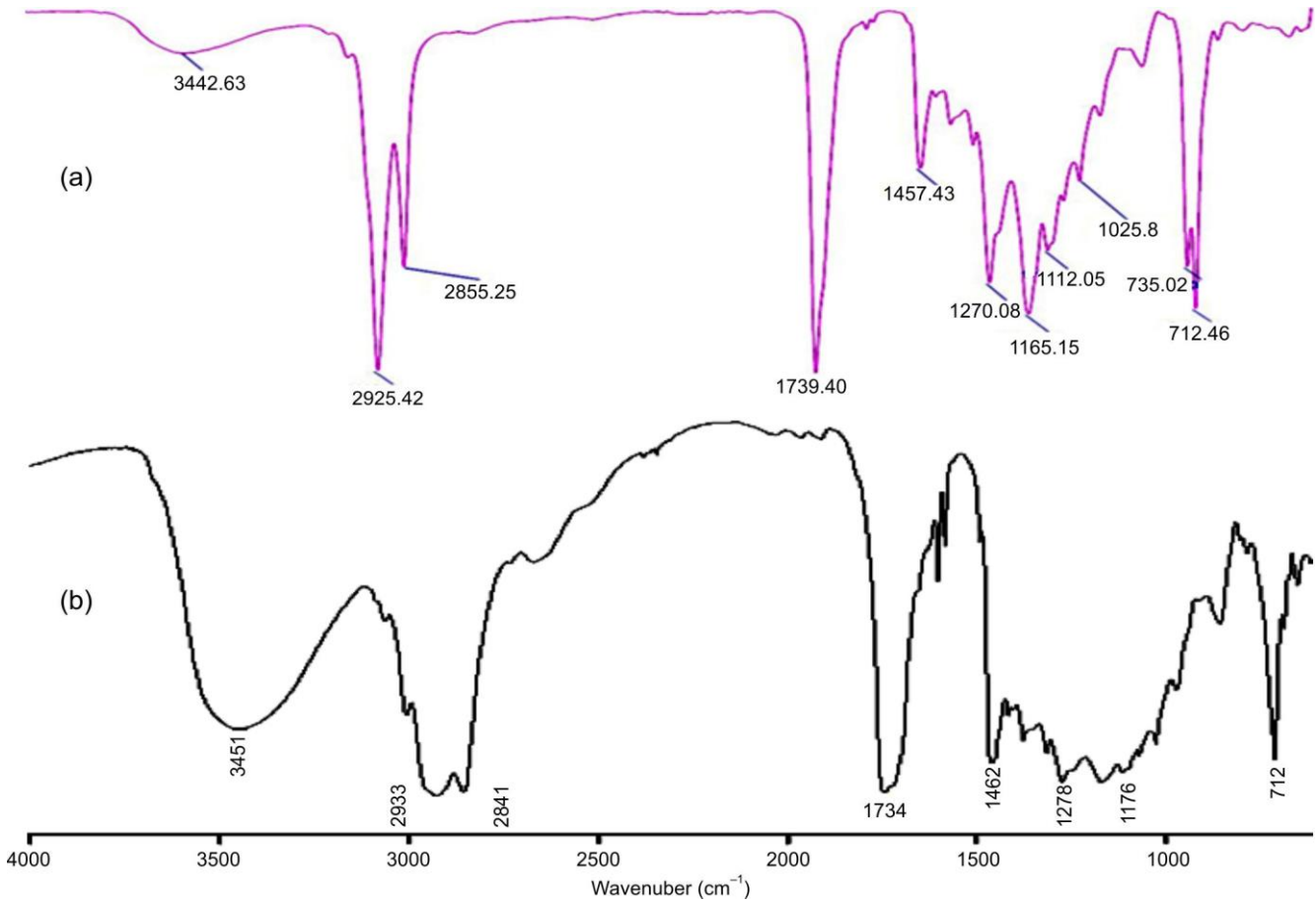

Fig. 1. FT-IR spectra of (a) polymer and (b) polymer/Fe_3O_4 nanocomposite

the ester carbonyl absorption shifts in polymer/nanocomposite. This shift may indicate an interaction between the polymer and nano-magnetite. Peaks at 1457, 1462, 1270 and 1278 cm^{-1} are attributed to the asymmetric and symmetric bending vibrations of C–H bonds in $–CH_3$ and $–CH_2–$ groups in a and b. Peaks in the range of 1165, 1176 and 1025 cm^{-1} correspond to the C–O stretching vibrations of the carboxylate ester group. A peak around 735 and 712 cm^{-1} represents the C–H bending vibrations in the paraffinic chain. Broad peaks observed at 2925 and 2933 cm^{-1} are due to the stretching vibrations of C–H bonds in $–CH_2–$ groups. Furthermore, the absence of significant peaks in the olefinic bond range supports the formation of the polymer.

The ^{1}H NMR spectra of the polymer and its nanocomposites representing the polymer and (B) corresponding to its nanocomposites (Fig. 2). In spectrum (A), a broad singlet between 3.99 to 4.14 ppm is attributed to the protons of the $–OCH_2$ group in the polymer. The methyl protons of the polymer chain appear around 0.76 ppm, while the absence of a singlet in the 5.5 ppm to 6.0 ppm range confirms the lack of any vinylic protons in the polymer. For nanocomposite, spectrum (B) shows a peak at 3.98 ppm corresponding to the $–OCH_2$ group protons. Methyl and methylene protons appear within the 0.77-1.90 ppm range, while a peak at 2.14 ppm corresponds to the protons of α-carbons adjacent to the ester carbonyl group. In ^{13}C NMR spectrum of the polymer, the carbonyl carbon appears at 174.3 ppm, with other sp^3 carbons in the 64.72 to 13.94 ppm range (Fig. 3a). For nanocomposites, the carbonyl carbon shifts slightly to 171.93 ppm as seen in spectrum (a). Peaks between 14.38 ppm and 40.44 ppm correspond to the sp^3 carbons of the alkyl chains in the nanocomposites (Fig. 3b). The reduced intensity of the NMR signals for the polymer composite is likely due to the interference of microwave frequencies with the magnetic material present in the composite. These results are in conformity with the previously findings [34].

Molecular weight: Gel permeation chromatography (GPC) was employed at room temperature in HPLC grade THF to determine the weight-average (M_w) and number-average (M_n) molecular weights of the synthesized polymers as shown in Table-1. The experimental results revealed that the prepared polymers exhibit a high molecular weight [38].

Thermogravimetric studies: The TG analysis of the polymer (P) and polymer/Fe_3O_4 nanocomposites (P-1), as illustrated in Fig. 4, indicates that incorporating nano-Fe_3O_4 enhances the thermal stability of the nanocomposites. At 250 ºC, the degradation percentages of polymer and polymer/Fe_3O_4 nanocomposites were measured as 29.45% and 14.67%, respectively. Similarly, at 350 ºC, the weight lost of polymer and polymer/Fe_3O_4 nanocomposites were estimated as 92.61% and 69.57% respectively. Hence, the presence of nano-Fe_3O_4 effectively slowed down the degradation process

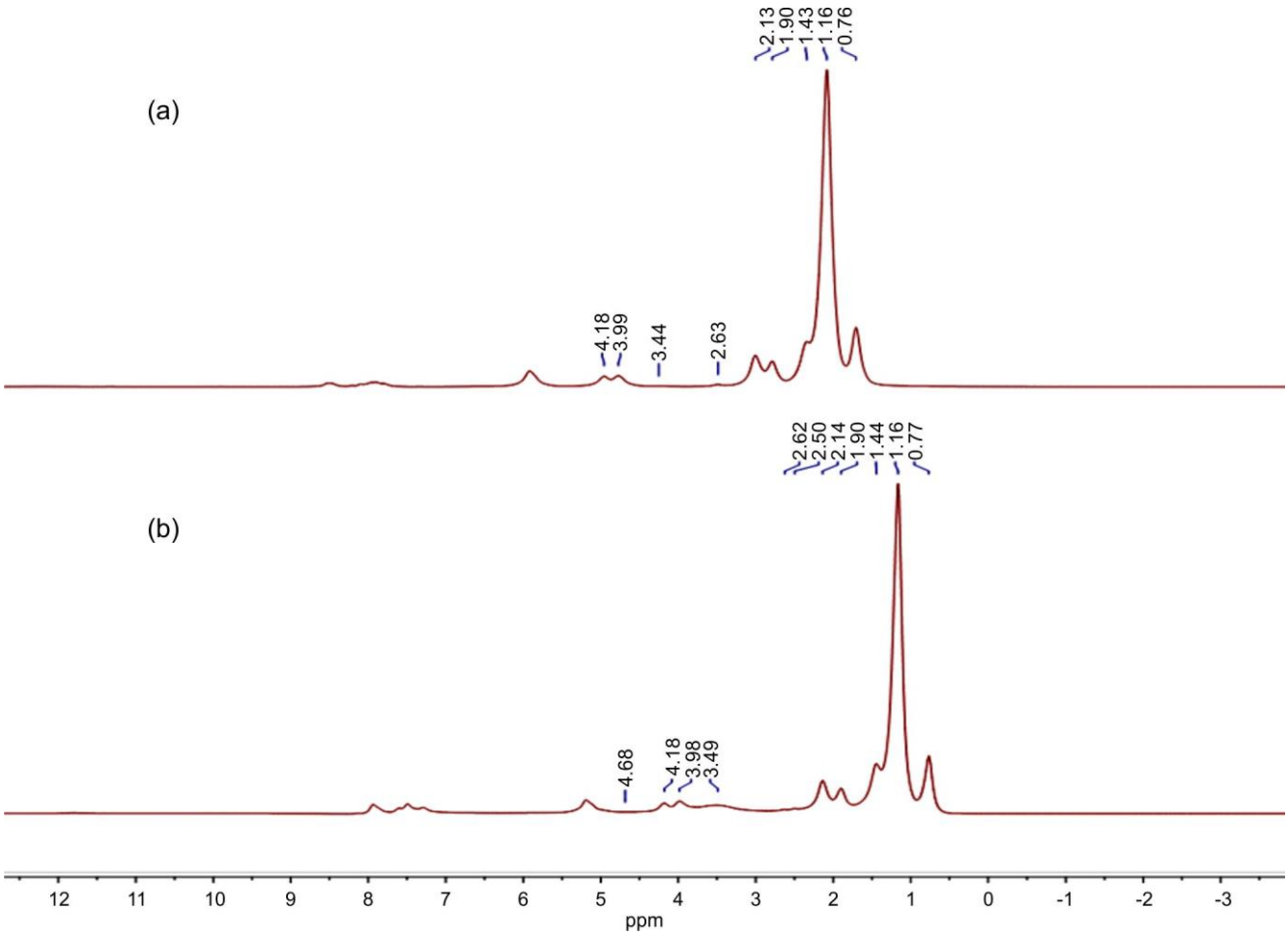

Fig. 2. ^{1}H NMR spectra of (a) polymer and (b) polymer/Fe_3O_4 nanocomposite

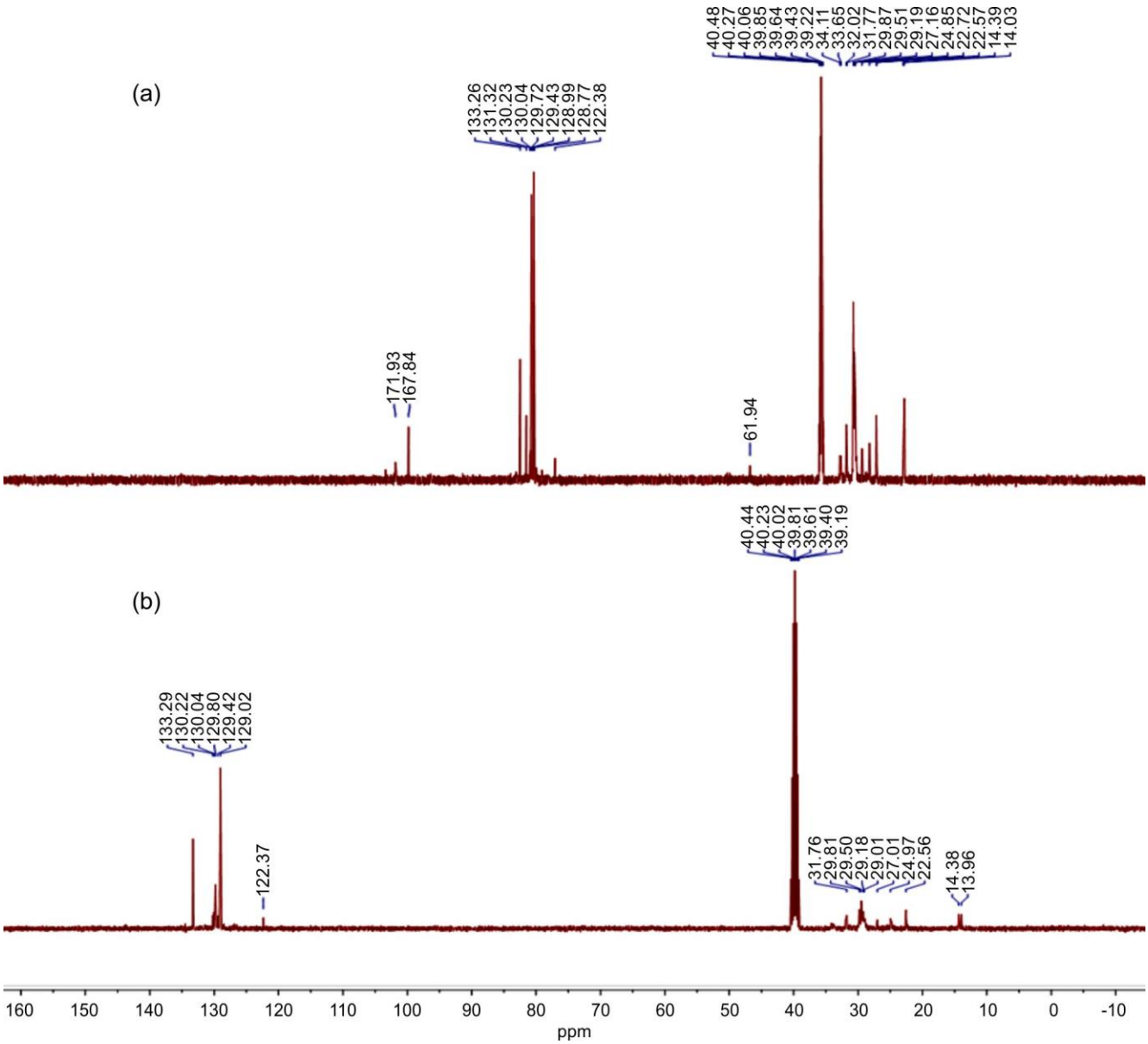

Fig. 3. ^{13}C NMR spectra of (a) polymer and (b) polymer/Fe_3O_4 nanocomposite

of the polymer, leading to improved thermal stability in the polymer composites [36].

XRD studies: The crystal structure of the synthesized Fe_3O_4 nanoparticles was analyzed using the XRD technique and is shown in Fig. 5, which was recorded over the 2θ range of 10º to 90º. The four most prominent peaks were observed at 30.4º, 32.0º, 43.7º and 67.9º, corresponding to the (220), (111), (400) and (207) crystal planes, respectively. These peaks closely resemble those reported for magnetite nanoparticles in other studies [33]. Additional peaks present in the pattern may indicate the presence of impurities.

SEM/TEM studies: Figs. 6 and 7 display the typical SEM and TEM images of the synthesized Fe_3O_4 nanoparticles respectively. The images reveal that most of the particles exhibit a mix of shapes, including spherical forms and flat, flake-like structures with smooth surfaces. Their sizes range from 20 nm to 75 nm. The crystalline characteristics of the Fe_3O_4 nanoparticles was further analyzed using FETEM

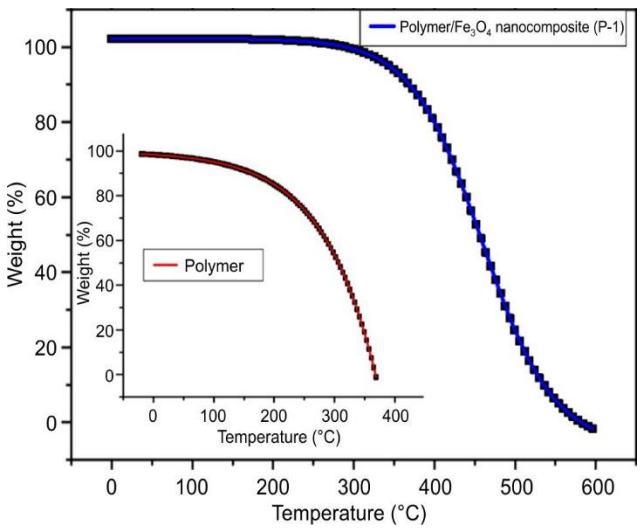

Fig. 4. TGA of polymer (P) and polymer/Fe_3O_4 nanocomposite (P-1)

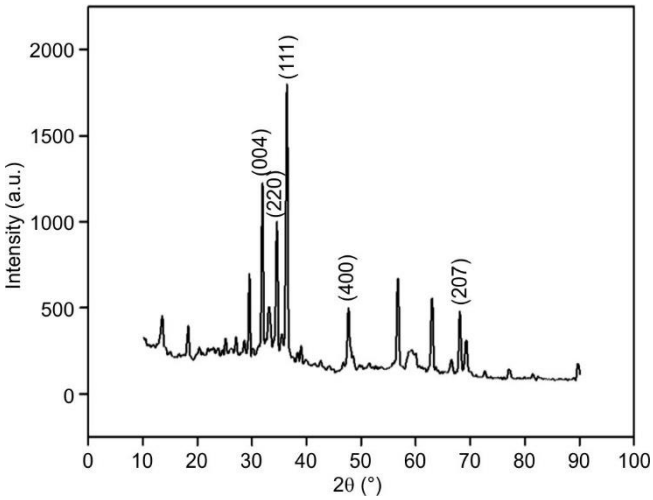

Fig. 5. XRD spectrum of prepared nano-Fe_3O_4

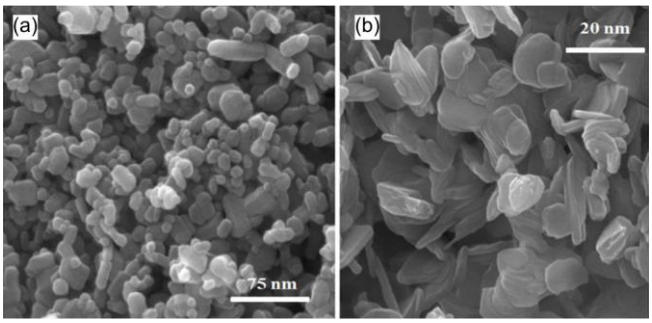

Fig. 6. SEM images of the prepared nano-Fe_3O_4

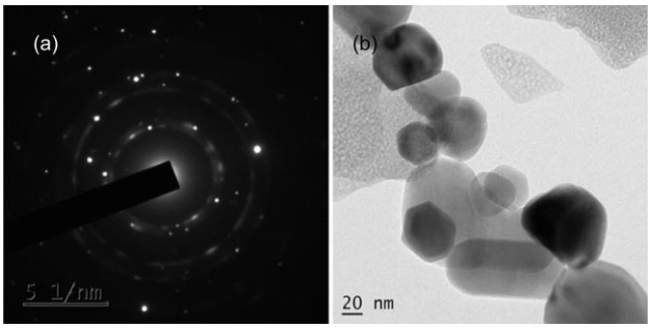

Fig. 7. TEM images of the prepared nano-Fe_3O_4

through electron diffraction patterns. Fig. 7a presents the selected area electron diffraction (SAED), indicating the polycrystalline nature of the synthesized nanoparticles.

Viscosity index (VI) values: The viscosity index (VI) values of the base oil blended with the polymer/nano-Fe_3O_4 composites (P-1, P-2 and P-3) outperform those of the pure polymer (P) at all concentrations (Table-2). The viscosity index (VI) consistently increases as the concentration of polymer/nano-Fe_3O_4 composites in the base stock increases as shown in Fig. 8. Among the samples, the lubricant containing 4% (P-3) additive exhibited the most significant improvement in the viscosity index compared to the rest of the base oil. This can be attributed to the increased total volume of polymer micelles in the lubricant as the additive concentration grows. Furthermore, the nanoparticles help separate the polymer chains within the matrix, further increasing the overall volume. This expanded volume of composite units in

TABLE-2
VISCOSITY INDEX OF LUBE OIL BLENDED WITH ADDITIVES AT VARYING CONCENTRATION LEVELS

Polymer code	Additive concentration (w/w)				
	0%	1%	2%	3%	4%
P	83	98	108	114	127
P-1	83	112	124	135	139
P-2	83	120	136	148	153
P-3	83	130	152	161	168

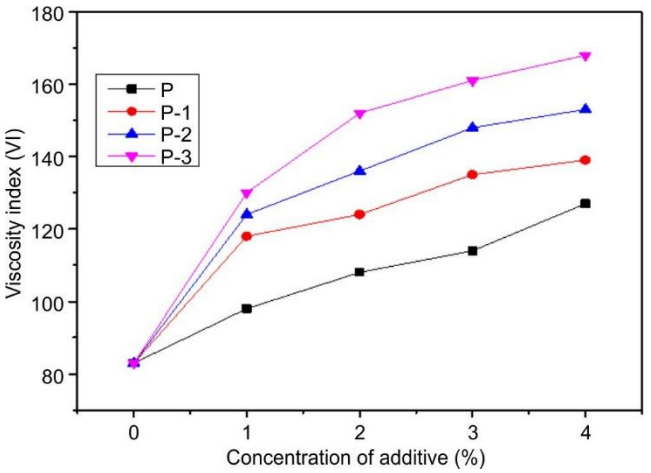

Fig. 8. Plot of viscosity index of lubricant oil blended with additives at various concentration levels

the solution ultimately leads to a higher viscosity index for the lubricant [39].

Pour point depressant (PPD): The PPD of lubricant compositions containing additives at varying concentrations (0 to 4 wt.%) was evaluated and the values are shown in Table-3. The findings demonstrate that the additives (P, P1, P2 and P3) effectively act as pour point depressants (PPDs). Among these, polymer P-3 exhibited the most outstanding PPD performance, surpassing P, P-1 and P-2 (Fig. 9). The ability of these polymers to lower pour points was significant, with their effectiveness increasing as the polymer concentration rose to 4%. This indicates that at this optimal concentration, the polymer interacts more efficiently with the paraffinic wax in the base oil, resulting in a reduction in the size of the wax crystals [40,41].

TABLE-3
POUR POINT OF BASE OIL BLENDED WITH ADDITIVES AT DIFFERENT CONCENTRATIONS (w/w)

Polymer code	Additive concentration (w/w)				
	0%	1%	2%	3%	4%
P	-6	-6.5	-7.0	-8.5	-10.0
P-1	-6	-8.5	-9.5	-10.5	-13.0
P-2	-6	-10.0	-11.0	-12.0	-14.0
P-3	-6	-10.0	-12.0	-12.0	-14.5

Anti-wear property: The tribological characteristics of the lubricant formulations (P, P-1, P-2 and P-3) were evaluated by measuring the wear scar diameter (WSD) using the four-ball wear test (FBWT) apparatus under a 392 N load. The addition of polymer/nanocomposites to the lubricant significantly enhances its anti-wear properties, as evidenced

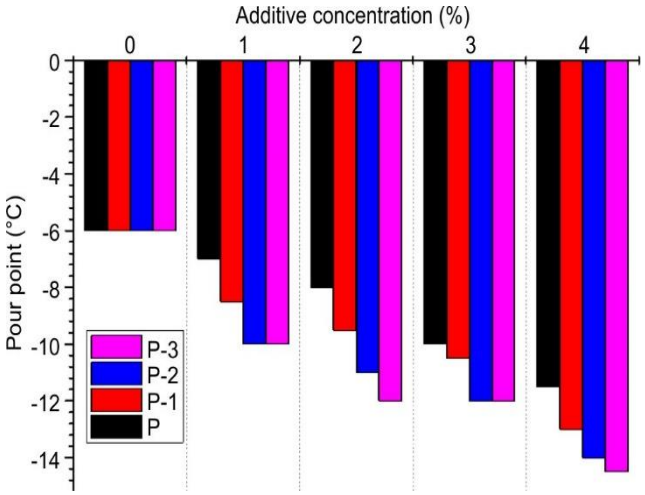

Fig. 9. Plot of pour points of lubricant oil blended with additives at varying concentration levels

by the reduced WSD values observed in the blended lubricant compositions (Table-4). The polymer P-3, at a 4% concentration, exhibited the most significant reduction in WSD values among all the polymers as shown in Fig. 10, which suggests that the lubricant forms a strong film between the two interacting metal surfaces. This effect could be attributed to a greater number of polar side chains, including ester carbonyl and hydroxyl groups present in castor oil [42].

TABLE-4
ANTIWEAR PROPERTY IN TERMS OF WEAR SCAR DIAMETER (WSD IN mm) VALUES OF DIFFERENT LUBRICANT COMPOSITION

Polymer code	WSD of lubricant oil in mm at different additive concentration (w/w)				
	0%	1%	2%	3%	4%
P	1.118	1.099	1.078	1.062	0.010
P-1	1.118	0.950	0.841	0.822	0.800
P-2	1.118	0.910	0.789	0.765	0.744
P-3	1.118	0.750	0.731	0.718	0.700

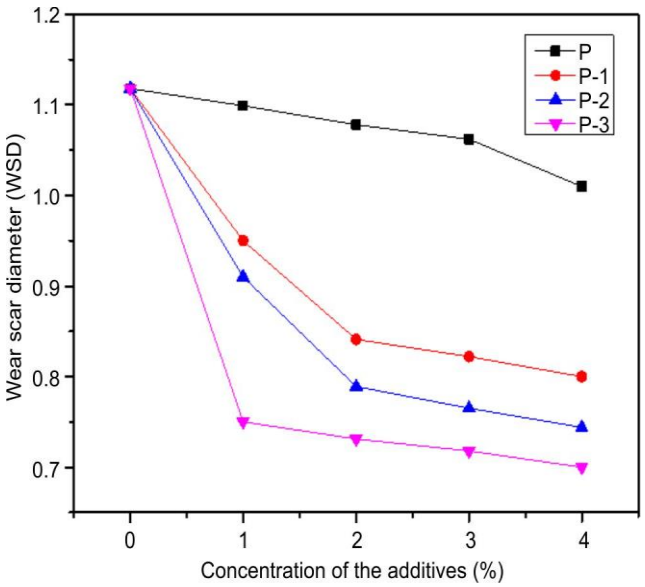

Fig. 10. Wear scar diameter (WSD) of the lubricant oil blended with additives at different percentage (w/w)

Conclusion

The research findings indicated that the synthesized nano-Fe_3O_4 can be incorporated as filler particle into polymer nanocomposites. The characterization of the polymer and the magnetite nanocomposites was conducted using XRD, SEM, TEM and various spectral analysis techniques. When evaluated as an additive in lubricants, the results showed that all the nanoblended composites enhanced the performance of the lubricant, acting as effective viscosity modifiers, pour point depressants and anti-wear. Consequently, this research presents a promising approach for designing multifunctional additives for lubricating oils.

CONFLICT OF INTEREST

The authors declare that there is no conflict of interests regarding the publication of this article.

REFERENCES

1. K. Holmberg and A. Erdemir, *Friction*, **5**, 263 (2017); https://doi.org/10.1007/s40544-017-0183-5
2. A. Elagouz, M.K.A. Ali, H. Xianjun, M.A.A. Abdelkareem and M.A. Hassan, *Surf. Eng.*, **36**, 144 (2020); https://doi.org/10.1080/02670844.2019.1620442
3. Z. Jiang, Y. Sun, B. Liu, L. Yu, Y. Tong, M. Yan, Z. Yang, Y. Hao, L. Shangguan, S. Zhang and W. Li, *Friction*, **12**, 1347 (2024); https://doi.org/10.1007/s40544-023-0808-9
4. Ú. Arinbjarnar, M. Moghadam and C.V. Nielsen, *Discov. Mechan. Eng.*, **3**, 6 (2024); https://doi.org/10.1007/s44245-024-00037-8
5. J. Li, T. Ren, H. Liu, D. Wang and W. Liu, *Wear*, **246**, 130 (2000); https://doi.org/10.1016/S0043-1648(00)00500-7
6. I.E. Uflyand, V.A. Zhinzhilo and V.E. Burlakova, *Friction.*, **7**, 93 (2019); https://doi.org/10.1007/s40544-019-0261-y
7. Deepika, *SN Appl. Sci.*, **2**, 1128 (2020); https://doi.org/10.1007/s42452-020-2916-8
8. W. Brostow, M. Dutta, J. Ricardo de Souza, P. Rusek, A. Marcos de Medeiros and E.N. Ito, *Express Polym. Lett.*, **4**, 570 (2010); https://doi.org/10.3144/expresspolymlett.2010.71
9. L. Sun, J. Zhou, Z. Zhang and H. Dang, *Wear*, **256**, 176 (2004); https://doi.org/10.1016/S0043-1648(03)00386-7
10. L. Rapoport, V. Leshchinsky, I. Lapsker, O. Nepomnyashchy, Y. Volovik, M. Lvovsky, R. Popovitz-Biro, Y. Feldman and R. Tenne, *Wear*, **255**, 785 (2003); https://doi.org/10.1016/S0043-1648(03)00044-9
11. Q. Xue, W. Liu and Z. Zhang, *Wear*, **213**, 29 (1997); https://doi.org/10.1016/S0043-1648(97)00200-7
12. A.I. Kuznetsov, V.A. Tyurikov and V.A. Kosmakov, *Chem. Heterocycl. Compd.*, **26**, 465 (1990); https://doi.org/10.1007/BF00497223
13. M.K.A. Ali, X. Hou and M.A.A. Abdelkareem, *Friction*, **8**, 905 (2020); https://doi.org/10.1007/s40544-019-0308-0
14. L. Duan, J. Li and H. Duan, *Friction*, **11**, 647 (2023); https://doi.org/10.1007/s40544-022-0667-9
15. B.Z. Wu, D. Wang, Y. Wang and A. Sun, *Adv. Eng. Mater.*, **12**, 534 (2010); https://doi.org/10.1002/adem.201000127
16. H.D. Huang, J.P. Tu, T.Z. Zou, L.L. Zhang and D.N. He, *Tribol. Lett.*, **20**, 247 (2005); https://doi.org/10.1007/s11249-005-8552-z
17. Y.Y. Wu, W.C. Tsui and T.C. Liu, *Wear*, **262**, 819 (2007); https://doi.org/10.1016/j.wear.2006.08.021
18. P. Uniyal, P. Gaur, J. Yadav, T. Khan and O.S. Ahmed, *ACS Omega*, **9**, 12436 (2024); https://doi.org/10.1021/acsomega.3c08279
19. J. Zhao, Y. Li, Y. He and J. Luo, *ACS Appl. Mater. Interfaces*, **11**, 36931 (2019); https://doi.org/10.1021/acsami.9b08993

20. Y. Wang, E. Forssberg, R.J. Pugh and S. Åke Elming, *J. Dispers. Sci. Technol.*, **16**, 137 (1995); https://doi.org/10.1080/01932699508943665
21. B. Li, X. Wang, W. Liu and Q. Xue, *Tribol. Lett.*, **22**, 79 (2006); https://doi.org/10.1007/s11249-005-9002-7
22. X. Xiong, Y. Kang, G. Yang, S. Zhang, L. Yu and P. Zhang, *Tribol. Lett.*, **46**, 211 (2012); https://doi.org/10.1007/s11249-012-9940-9
23. W. Huang, Æ.X. Wang, Æ.G. Ma and C. Shen, *Tribol. Lett.*, **33**, 187 (2009); https://doi.org/10.1007/s11249-008-9407-1
24. L. Xiang, C. Gao, Y. Wang, Z. Pan and D. Hu, *Particuology*, **17**, 136 (2013); https://doi.org/10.1016/j.partic.2013.09.004
25. A.M. Nassar, N.S. Ahmed, R.S. Kamal, A.-A.A. Abdel Azim and E.I. El-Nagdy, *Petrol. Sci. Technol.*, **23**, 537 (2005); https://doi.org/10.1081/LFT-200031097
26. G. Pranab, D. Tapan and D. Moumita, *J. Chem. Sci.*, **1**, 18 (2011).
27. P. Bataille, N. Sharifi-Sanjani and E. Evin, *J. Solution Chem.*, **23**, 325 (1994); https://doi.org/10.1007/BF00973553
28. M. Florea, D. Catrinoiu, P. Luca and S. Balliu, *Lubr. Sci.*, **12**, 31 (1999); https://doi.org/10.1002/ls.3010120103
29. E.B. Mubofu, *Sustain. Chem. Process.*, **4**, 11 (2016); https://doi.org/10.1186/s40508-016-0055-8
30. G. Karmakar and P. Ghosh, *ACS Sustain. Chem.& Eng.*, **3**, 19 (2015); https://doi.org/10.1021/sc500685r
31. G. Karmakar and P. Ghosh, *ACS Sustain. Chem.& Eng.*, **4**, 775 (2016); https://doi.org/10.1021/acssuschemeng.5b00746
32. I.J. Bruce, J. Taylor, M. Todd, M.J. Davies, E. Borioni, C. Sangregorio and T. Sen, *J. Magn. Magn. Mater.*, **284**, 145 (2004); https://doi.org/10.1016/j.jmmm.2004.06.032
33. W.L. Tan and M.A. Bakar, *J. Physiol. Sci.*, **17**, 37 (2006); https://doi.org/10.1142/9789812707307
34. K. Dey, G. Karmakar, M. Upadhyay and P. Ghosh, *Sci. Rep.*, **10**, 19151 (2020); https://doi.org/10.1038/s41598-020-76246-4
35. D.K. Saha and P. Ghosh, *J. Macromol. Sci. Part A Pure Appl. Chem.*, **55**, 384 (2018); https://doi.org/10.1080/10601325.2018.1444419
36. S. Tanveer and R. Prasad, *Indian J. Chem. Technol.*, **13**, 398 (2006).
37. M. Hoque, S. Paul and P. Ghosh, *J. Macromol. Sci. Part A Pure Appl. Chem.*, **58**, 329 (2021); https://doi.org/10.1080/10601325.2020.1854045
38. P. Ghosh, S. Talukder, M. Upadhyay and T. Das, *J. Sci. Ind. Res. (India)*, **75**, 420 (2016).
39. P. Ghosh and M. Das, *J. Chem. Eng. Data*, **58**, 510 (2013); https://doi.org/10.1021/je3008793
40. N.S. Ahmed, A.M. Nassar, R.M. Nasser, A.F. Khattab and A.A.A. Abdel-Azim, *Petrol. Sci. Technol.*, **26**, 1390 (2008); https://doi.org/10.1080/10916460701272195
41. I.M. El-Gamal, A.M. Atta and A.M. Al-Sabbagh, *Fuel*, **76**, 1471 (1997); https://doi.org/10.1016/S0016-2361(97)00062-8
42. C. Gao, Y. Wang, D. Hu, Z. Pan and L. Xiang, *J. Nanopart. Res.*, **15**, 1502 (2013); https://doi.org/10.1007/s11051-013-1502-z